J Mater Sci: Mater Med (2011) 22:1913–1922
DOI 10.1007/s10856-011-4366-8

Streptococcus sanguinis adhesion on titanium rough surfaces: effect of shot-blasting particles

Ana G. Rodríguez-Hernández · A. Juárez · E. Engel · F. J. Gil

Received: 19 August 2010 / Accepted: 30 May 2011 / Published online: 9 June 2011

Abstract Dental implant failure is commonly associated to dental plaque formation. This problem starts with bacterial colonization on implant surface upon implantation. Early colonizers (such as *Streptococcus sanguinis*) play a key role on that process, because they attach directly to the surface and facilitate adhesion of later colonizers. Surface treatments have been focused to improve osseointegration, where shot-blasting is one of the most used. However the effects on bacterial adhesion on that sort of surfaces have not been elucidated at all. A methodological procedure to test bacterial adherence to titanium shot-blasted surfaces (alumina and silicon carbide) by quantifying bacterial detached cells per area unit, was performed. In parallel, the surface properties of samples (i.e., roughness and surface energy), were analyzed in order to assess the relationship between surface treatment and bacterial adhesion. Rather than roughness, surface energy correlated to physico-chemical properties of shot-blasted particles appears as critical factors for *S. sanguinis* adherence to titanium surfaces.

A. G. Rodríguez-Hernández · F. J. Gil
Biomaterials, Biomechanics and Tissue Engineering Group, Department of Materials Science and Metallurgy, Universitat Politècnica de Catalunya, Avda. Diagonal 647, 08028 Barcelona, Spain

A. Juárez
Microbiology Department, Faculty of Biology, University of Barcelona, Av Diagonal 645, 08028 Barcelona, Spain

A. G. Rodríguez-Hernández (✉) · A. Juárez · E. Engel · F. J. Gil
Institut de Bioenginyeria de Catalunya (IBEC), Parc Cientific de Barcelona, C/Josep Samitier 1-5, 08028 Barcelona, Spain
e-mail: annroah@gmail.com

1 Introduction

Commercial pure Titanium (cp-Ti) and its alloys such as Ti–6Al–4V are widely used for dental implants because of their excellent osseointegration and mechanical properties. Improvements in these devices have led to increase their biological performance, where surface characteristics like roughness, wettability and surface energy have been widely studied in order to enhance cell response [1]. Topographical modifications to dental implants have shown that rougher surfaces obtained by several techniques on titanium implants (such as etching, sand blasting, etc.), presented a better osseointegration compared to smooth surfaces. This is due to the increased bone-implant contact area [2]. Human osteoblast cell adhesion on shot-blasted cp-Ti samples with alumina and silicon carbide has been evaluated, evidencing a good interaction due to both roughness ($R_a \approx 4$–5 μm) and composition of particles used [3]. A differential osteoblasts response (MG63) on that rough titanium surfaces was observed by Pegueroles et al. [4], where a better cellular response and extracellular matrix spatial organization on alumina shot-blasted compared to silicon carbide shot-blasted surfaces was observed. This might be associated to either particle presence (conformed part of topography) or changes caused by particle impact on surface. However, bacterial adhesion behaviour and biofilm formation to these surfaces has not been yet clarified.

Although titanium dental implants have presented good results in dental rehabilitation, there have been some problems associated to bacterial colonization either immediately upon implantation or after osseointegration. These problems are directly associated to dental plaque (inherent problem into human mouth). In the first case, bacteria commonly termed early colonizers (such as

Streptococcus sanguinis among others strains) [5–7] might be introduced into alveolar bone during surgery, attaching directly to implant body, resulting in inflammation that can lead to implant failure. In the second case, bacterial adhesion and colonization of the implant starts at surface irregularities, spreads into soft tissue (being this the main reason for using smooth surfaces in contact with oral fluids such as saliva and crevicular liquid), and results in a localized reaction, which may irreversibly damage implant surrounding tissues. In addition, the surface irregularities protect colonized bacteria from natural removal forces (salivary fluid flow, tongue and muscles action called *"self-cleaning"*), being that the reason why rough surfaces are directly associated with increased bacterial accumulation and higher incidence of peri-implantar disease [8]. When this illness becomes a chronic affection, it can lead to implant device failure.

Several studies about bacterial adhesion and dental plaque formation, either over teeth or dental material surfaces with a wide chemical composition had been performed in patients [9–11]. Where bacterial adhesion to solid surfaces appears to be influenced on many factors including: surface free energy, surface chemistry, surface charge, roughness or presence of proteins. These studies have been showed a significant correlation between some surface properties mentioned previously and its plaque-retaining capability [9, 12]. However, in vivo experimental studies of natural dental plaque are restricted both due to ethical issues and to the fact that dental plaque may greatly differ (biodiversity, heterogeneity, metabolic interaction and spatial organization) among individuals [13]. In addition, in the human mouth there are several dynamic mechanisms that act almost simultaneously (i.e. salival secretion, pH variations associated to metabolic bacterial activity, salivary fluid flow, etc.), and are involved in dental plaque formation, thus complicating the study of initial adhesion process.

In vitro adhesion experiments have also been developed in order to study bacterial colonization on titanium surfaces [11, 14–18], performing a pre-coating with human saliva. Nevertheless, these experiments presented several problems correlated to the heterogeneity of human saliva composition (such as ions, proteins, peptides, rheological properties, enzymes, etc.), even in the same person [19, 20]. Therefore, the fact to simulate in vivo conditions (with human saliva surface pre-coating) may mask the basic initial interaction of bacterial cells with the titanium surface.

In this work we have evaluated alumina and silicon carbide shot-blasted titanium properties (such as roughness and surface energy) and their effect on *S. sanguinis* attachment behaviour by using an in vitro adhesion assay in the optimal bacterial culture conditions.

2 Materials and methods

2.1 Titanium surfaces

Seven sorts of cp-Ti grade 2 rough surfaces were used. Basically, samples can be divided in two groups, shot-blasted and not shot-blasted samples. In the first group, disks (5 mm of diameter and 2 mm of thickness) were shot-blasted with aluminum oxide (Al_2O_3) and silicon carbide (SiC) with three different particles sizes (Table 1). In the second group a smoother surface (as bacterial adhesion negative control) was used. Flat surface was utilized directly once disks were cut.

2.2 Roughness

Roughness was analyzed with Interferometer Microscope, Optic Profiling System WYKO NT1100 (software Vision 32 from Veeco Metrology Group), where the surface area observed and analyzed was 604.4 × 459.9 μm for all samples. Three measurements were performed in three samples of each sort of treatment, obtaining the roughness average (Ra) and the index area (r) showed in Eq. 1:

$$r = \frac{\text{real area}}{\text{geometric area}} \tag{1}$$

where real area is the whole area of the surface and geometric area is correlated to surface measured in the projection plane.

2.3 Wettability and surface energy

To determine the surface energy we first evaluated the wettability. Contact angle was performed using Contact Angle System OCA from dataphysics Instruments with CCD equipment coupled and analyzed with software (SCA20). Ten measurements of each treatment were obtained from five samples at room temperature (T ≈ 25°C). Our samples presented non-flat surfaces, hence Young–Laplace equation is not the most appropriate to evaluate the wettability on that sort of samples, because it has been demonstrated the influence of heterogeneous surfaces (due to roughness, different phases or different materials conforming the whole topography) on contact angle. On those surfaces, the possibility to trap air into the grooves might lead to obtain incorrect measurements. There are contact angle corrections applied to rough and heterogeneous surfaces such as Casie-Baxter equations [21], where surface area in contact to liquid and air could be analyzed; the CCD resolution did not allow calculating them. The Wenzel correction [22] makes it possible to obtain the apparent contact angle, if the total surface is in contact with liquid. In order to fill all the grooves on rough

Table 1 Titanium surfaces used in this work

Nomenclature	Shot-blasting particle size (μm)
Flat	–
Al2	Al_2O_3 (212–300)
Al6	Al_2O_3 (425–600)
Al9	Al_2O_3 (1000–1400)
SI2	SiC (212–300)
SI6	SiC (425–600)
SI9	SiC (1000–1400)

Table shows, particle's size and composition for shot-blasting process

surfaces, we performed one variation of the sessile drop technique analysing the stabilized contact angle after injection (or advancing contact angle) in order to maintain the surface complete air bubble free (problem associated to sessile drop technique on rough surfaces). Then, we introduced the roughness (r) effect on wettability applying Wenzel equation to initial measurements (Fig. 1).

Finally, the surface energy and its polar and dispersive components were calculated with advancing contact angle results from three liquids with different surface tension (water, formamide and di-iodomethane) on each sort of rough surface using the Owens, Wendt, Rabel, Kaelble (OWRK) method [23–25]. In their theory they explain that polar and disperse contributions to the surface energy and surface tension are combined by forming the sum of both parts. Therefore one obtains:

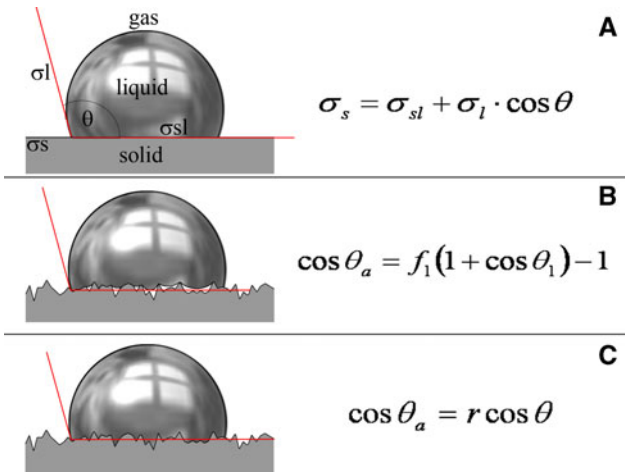

Fig. 1 Wettability equations used for surface energy calculation. Young–Laplace equation (**a**) is applied when surface sample is flat and homogeneous, whereas Casie-Baxter (**b**) considered a drop interaction between surface and bubble air (caught into roughness) as mixed surface. Finally Wenzel equation (**c**) considers surface depressions totally filled with liquid and made a total drop-contact surface area calculation introducing the roughness factor

$$\sigma_l = \sigma_l^d + \sigma_l^p \quad \sigma_s = \sigma_s^d + \sigma_s^p \tag{2}$$

where σ_l^d and σ_l^p represent disperse and polar parts of the liquid, while σ_s^d and σ_s^p stand for the respective contributions of the solid. At the same time, σ_{sl} is obtained from the contributions of the liquid and solid, forming the geometric mean.

$$\sigma_{sl} = \sigma_s + \sigma_l - 2\left(\sqrt{\sigma_s^d \cdot \sigma_l^d} + \sqrt{\sigma_s^p \sigma_l^p}\right) \tag{3}$$

Substituting this term for σ_{sl} in Young's equation (Eq. 4)

$$\sigma_s = \sigma_{sl} + \sigma_l \cdot \cos\theta \tag{4}$$

and rearranging the resulting expression into a general equation for a straight line ($y = a \cdot x + b$), one obtain the Eq. 5.

$$\frac{(1+\cos\theta)\sigma_l}{2\sqrt{\sigma_l^d}} = \sqrt{\sigma_s^p}\sqrt{\frac{\sigma_l^p}{\sigma_l^d}} + \sqrt{\sigma_s^d} \tag{5}$$

Then, by plotting y versus x from liquids analyzed (were necessary at least three liquids with different surface tension values, in order to achieve an adequate linear fit), we obtained σ_s^p from the slope of the fitted line and σ_s^d from the intersection with y axis.

2.4 Bacterial strains and growth conditions

Bacterial attachment experiments were performed with *S. sanguinis* strain CECT 480, supplied by Colección Española de Cultivos Tipo (CECT). Cells were routinely grown and maintained in Tood-Hewitt broth.

2.5 Surface energy evaluation of *S. sanguinis*

Microbial adhesion to solvents (MATS) is a simplified method to characterize the electron donor/electron acceptor properties of microbial cells, which in turn is a good parameter used to predict bacterial adhesion to solid surfaces in an aqueous environment [26]. Surface energy of bacterial strains was evaluated according to an adaptation of the MATS test [12]. Briefly, bacteria were collected during exponential growth phase, centrifuged (4000 rpm, 15 min, 4°C), washed twice with PBS 1× (Phosphate Buffer Solution) and finally resuspended in PBS 1×. Three different solvents were used: chloroform, hexane, and diethyl ether. 3 ml of bacterial suspension were placed in nine glass tubes (10 mm of diameter) and 400 μl of the corresponding solvent were added (three samples for each solvent). Upon 10 min incubation at room temperature, samples were vortexed for 1 min and allowed to stay for 15 min. The aqueous phase was then removed and its optical density (A_1) was measured. The average adhesion to solvents was calculated as $(1 - A_1/A_0) \times 100$, where A_0 is PBS optical density.

2.6 Bacterial attachment to Ti-surfaces

Prior to use, cp-Ti disks were washed with distilled water, ethanol and acetone, dried at room temperature and autoclaved. Cp-Ti disks (4 samples for each roughness) were introduced in Eppendorf® tubes containing 1 ml *S. sanguinis* cultures (bacterial concentration about 10^9 ufc/ml) and incubated for 2 h at 37°C. To quantify bacterial cells adhered to the cp-Ti disks; they were washed twice with PBS 1× and then introduced in new Eppendorf® tubes containing 1 ml Ringer solution. Upon continued vortexing (5 min) viable cell counts in the supernatant were determined. Detached CFU's were quantified, and normalized as CFU's/mm^2 and plotted versus, roughness and surface energy.

2.7 SEM sample preparation

In order to corroborate bacterial adhesion on cp-Ti disks, samples previously incubated with *S. sanguinis* were rinsed with PBS 1× and fixed with 2.5% glutaraldehide for 20 min. OsO_4 was added to each surface in order to stain the cells. Then, several alcohol dilutions (50–100%) were applied for bacteria dehydration and conservation, finally a gold layer by sputtering was applied in order to improve the sample-electron beam interaction. The observation was performed by Scanning Electron Microscope (JEOL JSM 6400) at 20 keV.

2.8 Statistical analysis

Statistical results about bacteria experiments were expressed as mean and standard deviation, which was determined by ANOVA one way test. The level of significance was set at $P < 0.05$. Each data point represents the mean ± standard deviation of at least five independent experiments.

3 Results

3.1 Roughness

In this work we first characterized the physicochemical properties of the different titanium surfaces. As negative control for bacterial attachment, Flat surface was used. In addition, three rough shot-blasted titanium surfaces were studied (either alumina (Al2, Al6, and Al9) or silicon carbide (SI2, SI6, and SI9). To asses roughness we first imaged the profile. Figure 2 shows the different samples and their topographical variations, correlated to particle size used during shot-blasting process. We also obtained roughness average (Ra) in micrometrical scale and roughness factor (index area) (Table 2), where the roughness topography and real area increment were directly correlated to the increase in the size of particles used. The data obtained evidenced a higher roughness on alumina shot-blasted titanium surfaces compared to silicon carbide shot-blasted samples. The same trend was observed on either real area or roughness factor (index area), which indicates the roughness increment on surfaces.

3.2 Wettability

To evaluate wettability on different titanium surfaces, advancing contact angle images were obtained, as example, Fig. 3 shows just Al2 surface, evaluated with water. The contact angle evolution whereas liquid was filling the initial drop was determined (Fig. 3a). Following drop sequences was possible to observe the evolution (Fig. 3b–d) and variation of contact angle. Measurements obtained during assay (mean and standard deviation of 10 samples), from contact angle evolution and drop contact diameter on titanium surfaces, showed two different trends:

(1) Contact angle value on Flat surface was almost stabilized throughout experiments (Fig. 4a) while drop contact diameter was increased gradually (Fig. 4b).
(2) Contact angle on rough surfaces (we have represented only Al2 surfaces) presented a higher variation on the contact angle at the beginning of the experiment, getting a stabilized contact angle after 20 s of injection (Fig. 4c), while drop contact diameter values showed a constant increment during contact angle stabilization (Fig. 4d).

Once determined the established contact angle for each surface from three different liquids (Water, Di-iodomethane, Formamide), the apparent contact angle was calculated applying Wenzel correction to initial measurements from each liquid (Table 3).

3.3 Surface energy

Surface energy values were also obtained. Table 4 shows the total surface energy and their polar and dispersive components from all titanium samples calculated according to OWRK equation (mean and standard deviation). Total surface values presented an increment directly correlated to roughness (Ra) augmentation (Fig. 5).

3.4 Surface properties of *S. sanguinis* cells (MATS test)

Results of MATS (mean and its standard deviation) showed a microbial adhesion of *S. sanguinis* to chloroform (polar solvent) was strong (72 ± 2%), and low to diethyl ether (basic solvent) 16 ± 2%. This indicates that this

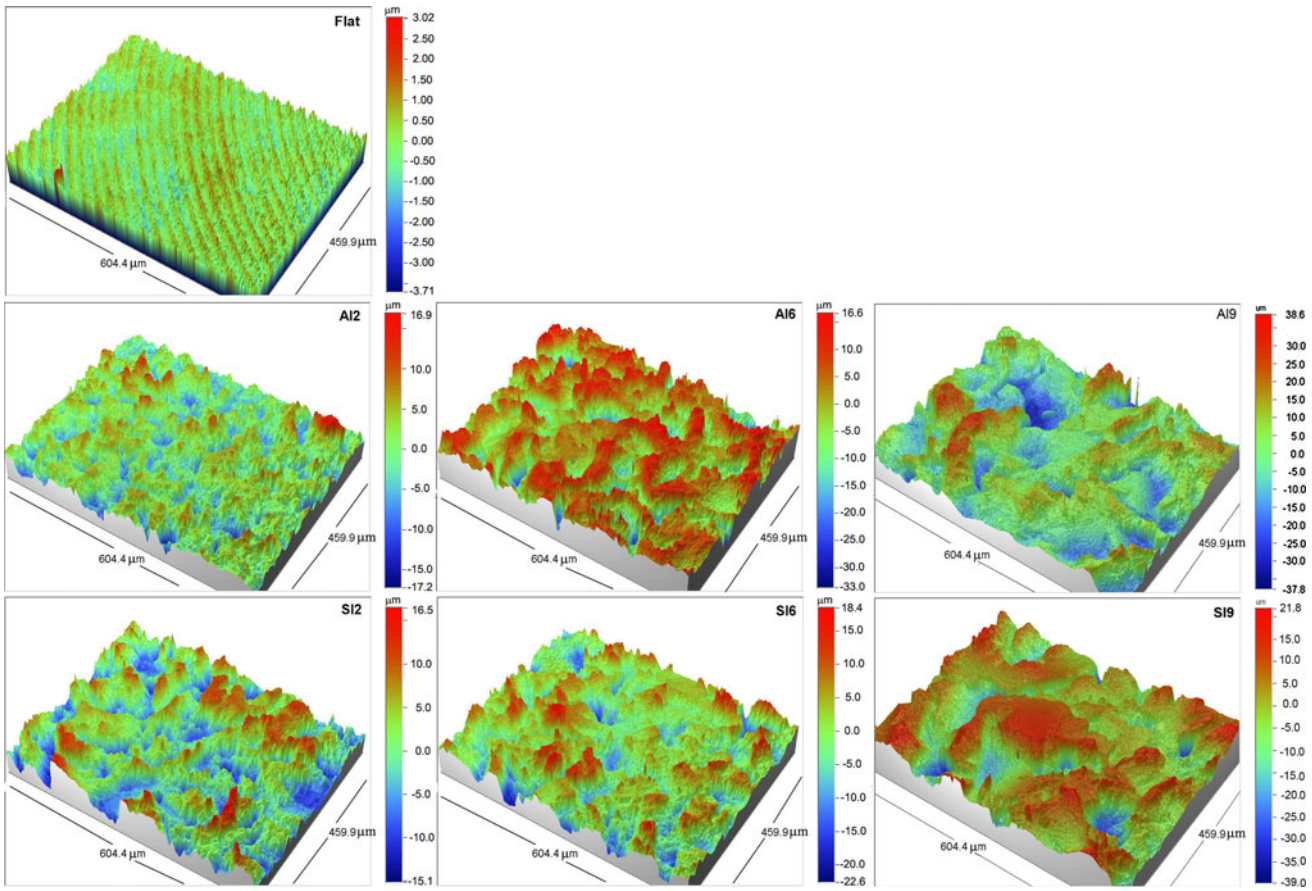

Fig. 2 Profiling images from titanium rough and smooth samples used in this work. Flat surface presented a Ra in nanometrical scales, whereas alumina and silicon carbide shot-blasted surfaces presented a micrometrical roughness. (See Table 2 for more details)

Table 2 Roughness (Ra) and index area (roughness factor) values from cp-Ti surfaces, obtained by interferometer microscope

Nomenclature	Roughness µm (Ra) ± SD	Index area ± SD	Nominal area (mm^2) ± SD	Real area (mm^2) ± SD
Flat	0.34 ± 0.03	1.06 ± 0.02**	70.7 ± 2	75 ± 2
Al2	2.9 ± 0.2**	1.6 ± 0.1*	70.7 ± 2	115 ± 4*
Al6	5.2 ± 0.6	1.8 ± 0.2*	70.7 ± 2	129 ± 3.5**
Al9	8 ± 1.4*	2 ± 0.5*	70.7 ± 2	144 ± 4
Sl2	2.7 ± 0.2**	1.3 ± 0.3**	70.7 ± 2	94 ± 2
Sl6	4 ± 0.4	1.7 ± 0.2*	70.7 ± 2	121 ± 3*
Sl9	7 ± 1.6*	1.8 ± 0.1*	70.7 ± 2	127 ± 2.5**

Values are means ± standard deviation, and statistical differences versus flat surfaces for each column are indicated by double and single asterisks

microorganism is a strong electron donor and weak electron acceptor. Furthermore, the fact that hexane-bacteria interaction was weak (13 ± 3%) indicates that *S. sanguinis* cells present a hydrophilic trend.

3.5 *Streptococcus sanguinis* adherence *to Ti-surfaces*

Once established the physicochemical properties of the different titanium surfaces, we assessed bacterial adherence to all of them. Adherence of *S. sanguinis* was first monitored by SEM (Fig. 6). It was possible to observe bacteria adhered to all different surfaces. However, cell imaging did not allow one to quantitate it. To achieve this, we used the *S. sanguinis* attachment protocol (see materials and methods for details). Attached bacterial cells were recovered from titanium disks by vortexing of previously rinsed samples and plate-counting (after seeding in Todd-Hewitt-agar) of cells released to the supernatant and normalized

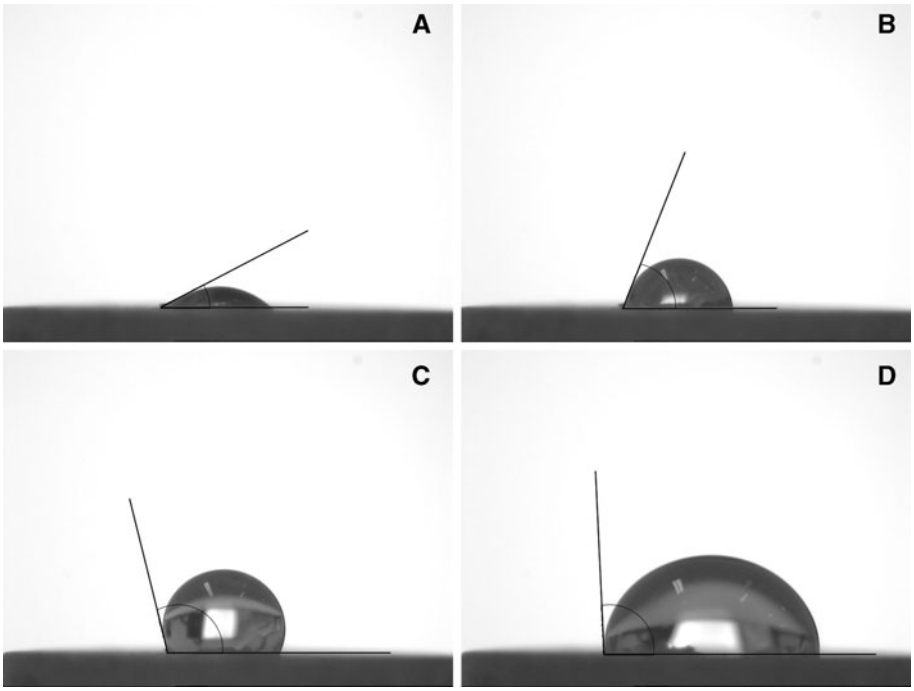

Fig. 3 Images of advancing contact angle on rough titanium surface (Al2), where the liquid quantity injected, is affecting the shape and angle of drop influenced by the sample topography

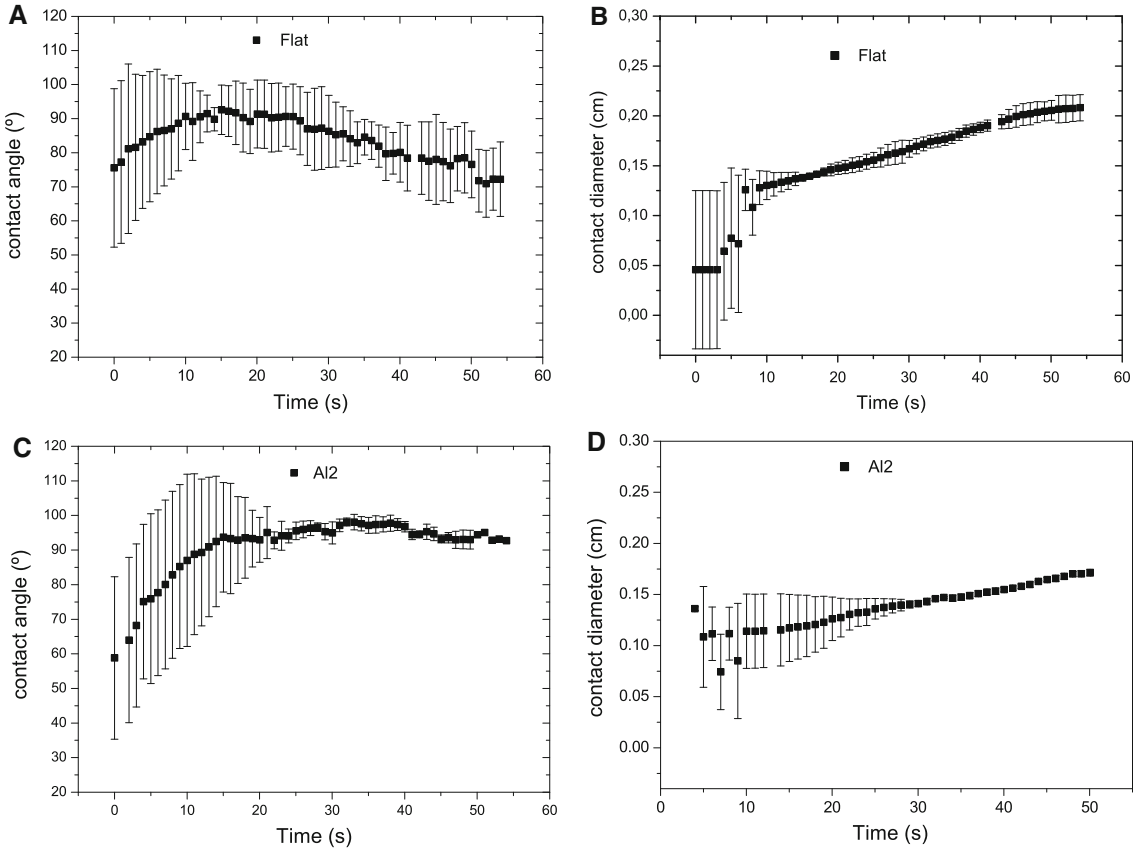

Fig. 4 Advancing contact angle results from Flat (**a**) and Al2 (**c**) surfaces, show the angle variation until their stabilization at 50 s, whereas **b** and **d** represent the drop contact area evolution respectively (all plotted points were mean and its standard deviation)

Table 3 Apparent contact angle for three different liquids obtained after Wenzel calculation (data represents mean and standard deviation)

Apparent contact angle (°)			
	Water	Di-iodometane	Formamide
Flat	83 ± 3	47 ± 5*	66 ± 4*
Al2	91 ± 5	33 ± 6**	68 ± 5*
Al6	66 ± 7**	16 ± 4	57 ± 8**
Al9	35 ± 6*	48 ± 2*	41 ± 3
SI2	49 ± 3	35 ± 7**	75 ± 8*
SI6	59 ± 5**	30 ± 3**	59 ± 6**
SI9	32 ± 3*	47 ± 6*	33 ± 3

Statistical differences versus Flat surfaces for each column are indicated by double and single asterisks

Table 4 Titanium surface energy values [total (σ_s), polar (σ_s^p) and dispersive (σ_s^d) components]

	Surface energy (mJ/m^2)		
	Dispersive component σ_s^d	Polar component σ_s^p	Total
Flat	32 ± 3*	4.6 ± 0.4*	36 ± 2
Al2	43 ± 4**	0.97 ± 0.02	44 ± 3**
Al6	40 ± 4 **	8.2 ± 0.4*	47 ± 4**
Al9	18 ± 3	35 ± 5	54 ± 5*
SI2	24 ± 4	17 ± 1	41 ± 3**
SI6	31 ± 3*	14 ± 1	45 ± 2**
SI9	50 ± 3	6 ± 3*	56 ± 5*

The values represented are mean and standard deviation and statistical differences versus Flat surfaces for each column are indicated by double and single asterisks

for area unity showed in Table 5 (mm^2) where mean and its standard deviation have been represented. Results obtained and plotted vs roughness and surface energy (Fig. 7), showed an increment in the amount of bacteria adhered when roughness increase, but this behaviour showed a very well defined trend associated to shot-blasted particle composition: when compared to silicon carbide shot-blasted surfaces, alumina shot-blasted samples presented a lower bacterial concentration per square millimetre adhered on their surface (one order of magnitude).

4 Discussion

The aim of this work was to evaluate the adherence of bacterial cells to rough titanium surfaces obtained by shot-blasting processes. Prior to this, a relevant aspect was to characterize the physicochemical properties of these surfaces. Surface energy determines the material surface-cell interaction, and the incorrect characterization of them might lead to wrong interpretations. Wettability values obtained by routinary sessil drop technique and used in order to calculate surface energy, did not allow one to establish any correlation between titanium surfaces and amount of adhered bacteria. We interpreted these data as the presence of air bubbles trapped into surface groves, rendering an incorrect wettability measurement, which in turn affects the surface energy results. However, a direct correlation between surface energy and roughness (Ra) was observed with results obtained from advancing contact angle measurements. These data show that surface energy increases proportionally to roughness values as should be expected.

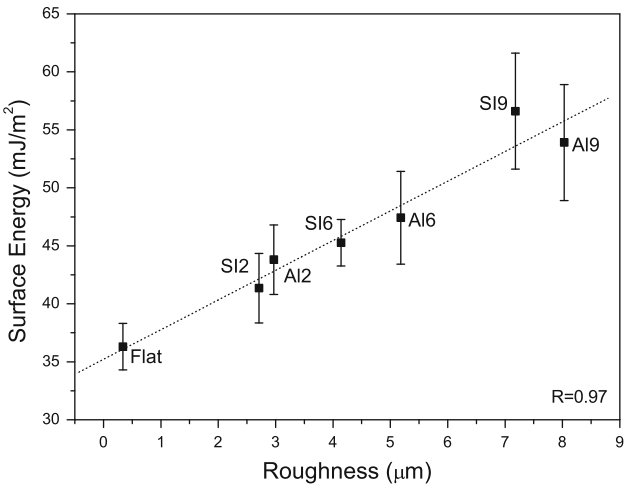

Fig. 5 Roughness plotted vs Surface Energy (mean and standard deviation), where increment on surface energy value was directly correlated to roughness increment, independent of shot-blasting particle used

Several authors [11, 27, 28] have not found a correlation between titanium surface energy and the degree of bacterial adhesion, concluding that bacterial attachment is more related to surface roughness. However, in our work we evidenced that *S. sanguinis* adhesion properties appear influenced for both roughness and surface energy related to surface treatment (Fig. 7). This last seems as critical parameter influencing bacterial adherence, because of bacterial cells showed a well defined sensitiveness correlated to shot-blasted particle used in order to modify the titanium surface, which is forming part of the titanium topography samples.

Different *S. sanguinis* adhesion trend observed in this work might be directly correlated to physicochemical properties of the particles used in order to increase titanium roughness. These intrinsic material properties to both alumina and silicon carbide, appears to have an influence on the fact observed in our results, where the highest amount of bacteria adhered to rough titanium was obtained in silicon carbide shot-blasted samples.

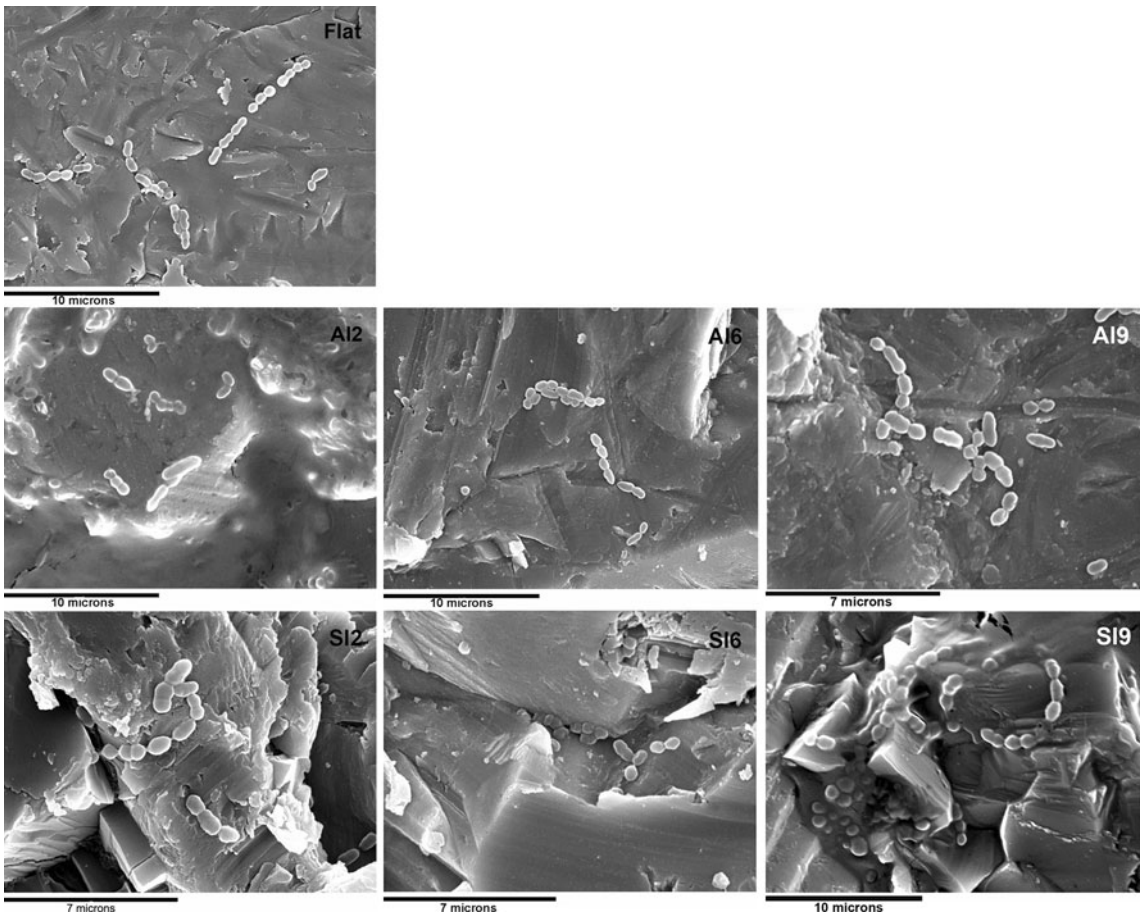

Fig. 6 Bacteria attached to different titanium rough surfaces observed by Scanning Electron Microscope

Table 5 Bacteria detached from all titanium surfaces and normalized per square millimetre (CFU/mm^2), measurements presented are mean and standard deviation

	Not shot-blasted	Shot-blasted					
	Flat	Al_2O_3			SiC		
		Al2	Al6	Al9	SI2	SI6	SI9
CFU/mm^2	$1.9 \times 10^2 \pm 9.2 \times 10^1$	$3.2 \times 10^2 \pm 2.3 \times 10^2$	$5 \times 10^2 \pm 8.5 \times 10^1$	$1.3 \times 10^3 \pm 9 \times 10^2$	$6.2 \times 10^2 \pm 3.4 \times 10^2$	$3.5 \times 10^3 \pm 1 \times 10^3$*	$1 \times 10^4 \pm 3 \times 10^3$*

Statistical differences versus flat surfaces are indicated by asterisk

According to Poortinga et al. [29], bacteria adhesion onto either conducting or semi-conducting materials (such as silicon carbide), was given by electron transfer from carboxylate functional groups in bacterial cell surface proteins to material surface. Both free electrons from bacteria cell (due to electron donor property of *S. sanguinis*, demonstrated with our MATS results) and free valence shell of silicon carbide were sharing electrons as adhesion mechanism. In silicon carbide, the basic unit of the crystal gave a reactive surface layer associated either silicon or carbon atoms [30]. These external faces (either carbon or silicon) may guide bacterial attachment behaviour providing a more reactive surface, due to presence of free valence shell.

Moreover, in aluminum oxide the unit cell is formed by ionic bond between aluminum and oxygen atoms from the transfer of electrons since one atom to another, then the valence shell is thereby filled, which might limit the bacterial adhesion to aluminum oxide shot-basted surfaces.

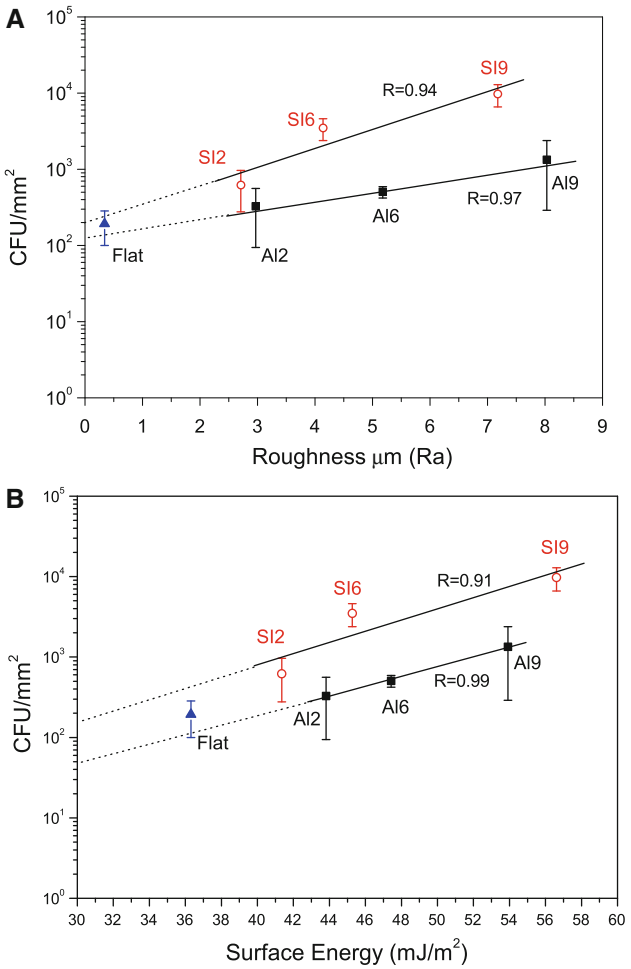

Fig. 7 CFU/mm^2 attached on titanium rough surfaces plotted versus roughness (**a**) and total surface energy (**b**), both graph shows a well defined difference between particle treatments, where alumina shot-blasted surfaces presented the lower quantity of bacteria adhered, compared to silicum carbide shot-blasted titanium surface. In the graph are plotted the mean and standard deviation

Although it cannot be ruled out, that different types of bacteria exhibit adherence properties different to those of *S. sanguinis*, the fact that this strain is an early colonizer of the dental plaque, makes our model as valuable and simplified model to test differential adherence to biomaterials used in dental implants. Hence, rather than roughness and surface energy, physicochemical properties of shot-blasted particles appear as critical factors for the *S. sanguinis* adhesion to titanium surfaces.

Furthermore, our studies have been shown how applying Wenzel correction to advancing contact angle results, let to obtain a better estimation of surface energy and its polar and dispersive components with a simplified methodology. This can be use in cell-biomaterials surface interaction studies as well as surface energy characterization of any sort of material which present a rough topography, when this property plays a key role.

5 Conclusions

From this work we can conclude that:

(1) The advancing contact angle and Wenzel correction applied in order to calculate the total surface energy used on rough surfaces, let to achieve a better surface energy characterization, because of air bubble free measurements obtained.
(2) Physicochemical properties of particles used for surface modification to titanium surfaces lead different bacterial adhesion.
(3) Alumina shot-blasted titanium surfaces, presented a lower amount of bacteria attached, compared to silicon carbide shot-blasted surfaces.

Acknowledgments Rodriguez-Hernández appreciates the financial support from CONACYT-México (Consejo Nacional de Ciencia y Tecnología). This study was supported by MICINN (Ministerio de Ciencia e Innovación) from Spanish Government, project: MAT2009-13547.

References

1. Eisenbarth E, Meyle J, Nachtigall W, Breme J. Influence of the surface structure of titanium materials on the adhesion of fibroblasts. Biomaterials. 1996;17:399–1403.
2. Lincks J, Boyan BD, Blanchard CR, Lohmann CH, Liu Y, Cochran DL, Dean DD, Schwartz Z. Response of MG63 osteoblast-like cells to titanium and titanium alloy is dependent on surface roughness and composition. Biomaterials. 1998;19:2219–32.
3. Aparicio C, Gil FJ, Peraire C, Padròs A, Planell JA. Abstract Booklet Titanium, 99. 2000;2:1207–10.
4. Pegueroles M, Aparicio C, Bosio M, Engel E, Gil FJ, Planell JA, Altankov G. Spatial organization of osteoblast fibronectin matrix on titanium surfaces: effects of roughness, chemical heterogeneity and surface energy. Acta Biomater. 2009;6:291–301.
5. Weiger R, Decker E-M, Krastl G, Brecx M. Deposition and retention of vital and dead *Streptococcus sanguinis* cells on glass surfaces in a flow-chamber system. Arch Oral Biol. 1999;44:621–8.
6. Rickard A-H, Gilbert P, High N-J, Kolenbrander P, Handley P-S. Bacterial coaggregation an integral process in the development of multi-species biofilms. Trends Microbiol. 2003;11:94–100.
7. Maeda K, Nagata H, Nonaka A, Kataoka K, Tanaka M, Shizukuishi S. Oral streptococcal glyceraldehydes-3phosphate dehydrogenase mediates interaction with *Porphyromonas gingivalis frimbria*. Microbes Infect. 2004;6:1163–70.
8. Norowski PA, Bumgardner JD. Review, Biomaterial and antibiotic strategies for Peri-implantitis. J Biomed Mater Res Part B Appl Biomater. 2009;88B:530–43.
9. Teughels W, van Assche N, Sliepen I, Quirynen M. Effect of material characteristics and/or surface topography on biofilm development. Clin Oral Implants Res. 2006;17:68–81.
10. Elter C, Heuer W, Demling A, Hannig M, Heidenblut T, Bach F, Stiesch-Scholz M. Supra and subgingival biofilm formation on implant abutments with different surface characteristics. Int J Oral Maxillofac Implants. 2008;23:327–34.
11. Bürgers R, Gerlach T, Hanhel S, Schwartz F, Handel G. Gosau. In vitro and in vivo biofilm formation on two different titanium implant surfaces. Clin Oral Implants Res. 2010;21:156–64.

12. Mabboux F, Ponsonnet L, Morrier J-J, Jaffrezic N, Barsotti O. Surface free energy and bacterial retention to saliva-coated dental implant materials-an in vitro study. Colloids Surf B Biointerfaces. 2004;39:199–205.
13. Sissons CH. Artificial dental plaque biofilm model system. Adv Dent Res. 1997;11:110–26.
14. Steinberg D, Sela M, Klinger A, Kohavi D. Adhesion of periodontal bacteria to titanium and titanium alloy powders. Clin Oral Implants Res. 1998;9:67–72.
15. Länge K, Herold M, Scheideler L, Geis-Gerstorfer J, Wendel HP, Gauglitz G. Investigation of initial pellicle formation on modified titanium dioxide (TiO_2) surfaces by reflectometric interference spectroscopy (RIFS) in a model system. Dent Mater. 2004;20:814–22.
16. Gerber J, Wenaweser D, Mayfield-Heitz L, Niklaus L, Persson G. Comparison of bacterial plaque samples from titanium and tooth surfaces by different methods. Clin Oral Implants Res. 2006;17:1–7.
17. Fürst M, Salvi G, Lang N, Persson G. Bacterial colonization immediately after installation on oral titanium implants. Clin Oral Implant Res. 2007;18:501–8.
18. Hauser-Gerspach I, Kulik E-M, Weiger R, Decker E-M, Von Ohle C, Meyer J. Adhesion of *Streptococcus sanguinis* to dental implant and restorative materials in vitro. Dent Mater J. 2007;26:361–6.
19. Schenkels L, Veerman E, Amerongen A. Biochemical composition of human saliva in relation to other mucosal fluids. Crit Rev Oral Biol Med. 1995;6:161–75.
20. Stokes J, Davies G. Viscoelasticity of human whole saliva collected after acid and mechanical stimulation. Biorheology. 2007;44:141–60.
21. Cassie BD, Baxter S. Wettability of porous surfaces. Trans Faraday Soc. 1944;40:546–51.
22. Wenzel R. Resistance of solid surfaces to wetting by water. Ind Eng Chem. 1936;28:988–94.
23. Owens D, Wendt R. Estimation of the surface energy of polymers. J Appl Polym Sci. 1969;13:1741–7.
24. Sharma P, Hanumantha R. Analysis of different approaches foe evaluation of surface energy of microbial cells by contact angle goniometry. Adv Colloid Interfaces Sci. 2002;98:341–463.
25. Pareta R, Reising A, Miller T, Storey D, Webster T. Increased endothelial cell adhesion on plasma modified nanostructured polymeric and metallic surfaces for vascular stent applications. Biotechnol Bioeng. 2009;103:459–71.
26. Bellon-Fontaine M-N, Rault J, van Oss CJ. Microbial adhesion to solvents: a novel method to determine the electron donor/electron acceptor or Lewis acid-base properties of microbial cells. Colloids Surf B Biointerfaces. 1996;7:47–53.
27. Quirynen M, van de Mei H, Bollen C, Schotte A, Marechal M, Doornbusch G, Naert I, Busscher H, van Steenberghe D. An in vivo study of the influence of the surface roughness of implants on the microbiology of supra- and subgingival plaque. J Dent Res. 1993;72:1304–9.
28. Größner-Schreiber B, Griepentrog M, Haustein I, Müller W, Lange K, Briedigkeit H, Göbel U. Plaque formation on surfaces modified dental implants, an in vitro study. Clin Oral Implant Res. 2001;12:543–51.
29. Poortinga A, Bos R, Busscher H. Charge transfer during staphylococcal adhesion to TiNOX® coatings with different specific resistivity. Biophys Chem. 2001;91:273–9.
30. Madar R. Silicon carbide in contention. Nature. 2004;430:974–5.